

Local structural disorder in REFeAsO oxypnictides by RE L₃ edge XANES

This article has been downloaded from IOPscience. Please scroll down to see the full text article.

2010 J. Phys.: Condens. Matter 22 125701

(<http://iopscience.iop.org/0953-8984/22/12/125701>)

[The Table of Contents](#) and [more related content](#) is available

Download details:

IP Address: 193.206.87.60

The article was downloaded on 09/03/2010 at 12:55

Please note that [terms and conditions apply](#).

Local structural disorder in REFeAsO oxypnictides by RE L₃ edge XANES

W Xu¹, A Marcelli², B Joseph³, A Iadecola³, W S Chu¹,
D Di Gioacchino², A Bianconi³, Z Y Wu^{1,4} and N L Saini³

¹ BSRF, Institute of High Energy Physics, Chinese Academy of Sciences, 10049, Beijing, People's Republic of China

² Laboratori Nazionali di Frascati, INFN, 00044 Frascati, Italy

³ Dipartimento di Fisica, Università di Roma 'La Sapienza', Piazzale Aldo Moro 2, 00185 Roma, Italy

⁴ NSRL, University of Science and Technology of China, Hefei 230026, People's Republic of China

Received 2 December 2009, in final form 16 January 2010

Published 8 March 2010

Online at stacks.iop.org/JPhysCM/22/125701

Abstract

The REFeAsO (RE = La, Pr, Nd and Sm) system has been studied by RE L₃ x-ray absorption near edge structure (XANES) spectroscopy to explore the contribution of the REO spacers between the electronically active FeAs slabs in these materials. The XANES spectra have been simulated by full multiple scattering calculations to describe the different experimental features and their evolution with the RE size. The near edge feature just above the L₃ white line is found to be sensitive to the ordering/disordering of oxygen atoms in the REO layers. In addition, shape resonance peaks due to As and O scattering change systematically, indicating local structural changes in the FeAs slabs and the REO spacers due to RE size. The results suggest that interlayer coupling and oxygen order/disorder in the REO spacers may have an important role in the superconductivity and itinerant magnetism of the oxypnictides.

1. Introduction

The recent discovery of high temperature superconductivity in iron-based oxypnictides (REFeAsO) [1] has triggered a large amount of research activity with a focus on the understanding of their fundamental properties and the underlying magnetic and structural order [2]. Incidentally, the structural topology of the oxypnictides is similar to the well-known cuprate superconductors, with electronically active FeAs layers separated by the REO spacers, as of the CuO₂ layers separated by the rock-salt reservoirs in the latter [3–7]. Another unifying link between the two families of materials is the appearance of superconductivity in the proximity of an antiferromagnetically ordered state [2, 8].

The REFeAsO becomes superconducting, with a maximum transition temperature $T_c \sim 55$ K [2], when the active FeAs layers are doped through atomic substitutions or oxygen vacancies in the REO spacers. In the superconducting system, the structural transition, as well as the magnetic order, disappear [2]. Since superconductivity and itinerant striped magnetism are known to occur in FeAs, most of the studies are focused on addressing the characteristics of the FeAs layers, overlooking the REO spacers. On the other hand, recent studies

on the cuprates have clearly underlined the importance of the spacer layers, in which the atomic order/disorder appears to have a vital role in their superconductivity [9, 10]. In addition, the misfit strain due to the spacer layer could easily modify the structural topology as well the atomic order, and hence the fundamental properties of the system [11]. In fact, while the maximum T_c of the doped system increases with reducing RE ion size [12, 13], the structural transition temperature (T_s) decreases for the undoped system [14, 15], underlying the importance of the local chemistry of the REO layers in the correlating itinerant magnetism and superconductivity of the oxypnictides. Moreover, Fe K edge EXAFS studies on the REFeAsO have revealed the strongly covalent nature of the Fe–As bond [16]. Indeed, the EXAFS results show that, depending on the RE size, the As atom changes its vertical position with respect to the Fe–Fe plane, indicating an increased interaction with the REO spacers [16]. Therefore, it is of prime importance to study the local structural characteristics of the spacer layer in order to explore its role in the itinerant magnetism and superconductivity of the oxypnictides.

X-ray absorption near edge structure (XANES) is a fast ($\sim 10^{-15}$) and local experimental technique (5–10 Å) capable of investigating the short/medium range order and electronic

structure of materials [17]. The x-ray absorption coefficient $\mu(E)$ is given by the product of the matrix element and joint (empty) density of states for the electronic transitions from the initial to the final states. The dipole matrix element from the initial state, the core level of well defined symmetry, selects the local and partial density of final states for the allowed electronic transitions. XANES spectroscopy probes the final states in an energy range of about 50–60 eV (depending on the system) above the chemical potential. The XANES spectra can be solved in real space, describing the final state as an outgoing spherical wave that interferes with the waves back-scattered from the neighboring atoms [18]. In particular, RE L_3 -edge XANES spectroscopy, being a direct probe of the local structure around the RE atom and the distribution of the valence electrons with the final states in the continuum being due to multiple scattering resonances of the photoelectron in a finite cluster [17], is an ideal tool to study local geometry around the RE and has often been applied to study RE containing materials [19–22].

In this work we have exploited RE L_3 -edge XANES spectroscopy in obtaining direct information on the local structure around the RE atom to study the role of the REO layer and its interaction with the FeAs layers in the REFeAsO (RE = La, Pr, Nd and Sm) oxypnictides. The multiple scattering theory has been employed to identify the nature of the different features and their evolution as a function of RE size. A systematic change in the spectral features can be observed, reflecting the varying electronic and local geometrical structure of the REOFeAs. In particular, the first near edge feature above the L_3 white line is found to be highly sensitive to the ordering of oxygen atoms, while the shape resonance peaks evolve systematically with the RE size. The results suggest that the misfit between the FeAs and REO layers [7, 11] and oxygen order/disorder in the REO spacers should have an important role to play in the superconductivity and itinerant magnetism of the oxypnictides.

2. Technical details

2.1. RE L_3 -edge x-ray absorption measurements

The x-ray absorption measurements were performed on powder samples of REFeAsO (RE = La, Pr, Nd, Sm) prepared using the solid state reaction method [23]. Prior to the absorption measurements, the samples were characterized by x-ray diffraction for their structural properties [14]. RE L_3 -edge x-ray absorption near edge structure (L_3 -XANES) measurements were performed at the XAFS beamline of the Elettra Synchrotron Radiation Facility, Trieste, where the synchrotron radiation emitted by a bending magnet source was monochromatized using a double crystal Si(111) monochromator. The transmission mode was used for the measurements, using three ionization chambers mounted in series for the simultaneous measurements on the sample and a reference. Several absorption scans were collected to ensure the reproducibility of the spectra and a high signal to noise ratio.

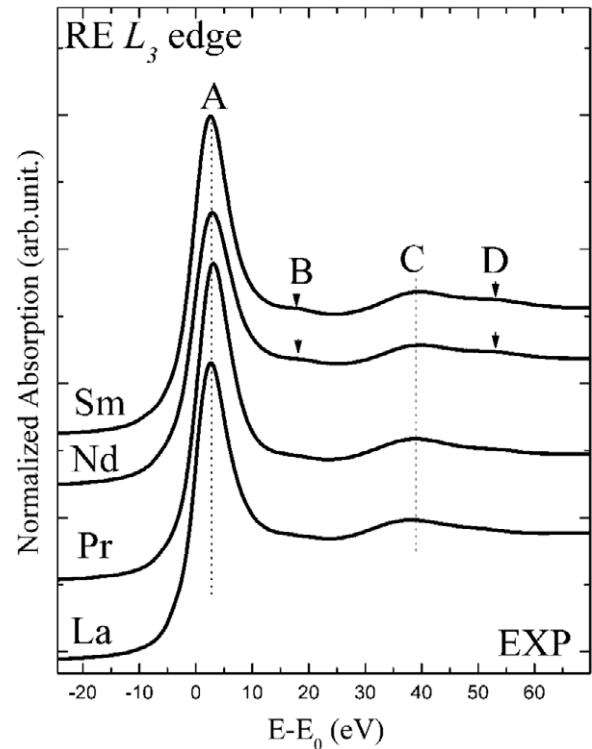


Figure 1. RE L_3 -edge x-ray absorption near edge spectra of REFeAsO (RE = La, Pr, Nd, Sm). In the near edge region, up to ~ 60 eV above the edge, all spectra shows four features. As the ionic radii increases, feature B gets more pronounced. The zero of the energy scale is fixed to the first derivative of the L_3 -edge.

2.2. Multiple scattering calculations

To understand the electronic structure of the system, we have performed systematic simulations over the rare-earth L_3 edges, using self-consistent real-space multiple scattering by the FEFF8.2 code [24, 25] within the muffin-tin approximation. The atomic potential is calculated self-consistently using a cluster of up to 127 atoms within a radius of 8.0 Å. The multiple scattering calculation converges when a cluster of 13 shells (59 atoms up to 6.15 Å) is considered. For the calculations, the energy and position dependent Hedin–Lundqvist optical potential [26] has been selected as the exchange–correlation potential. The total electronic potential was constructed by spherically averaging the muffin-tin potentials on each atom and keeping constant the potential in the interstitial region between the muffin-tin spheres. The f states for all the rare-earth metals were kept in a frozen state to achieve convergence of the self-consistent potentials ($l_{\max} = 3$). Once f states were allowed to be involved, the calculations showed a shift of 1 eV towards lower energy.

3. Results and discussion

Figure 1 shows experimental rare-earth L_3 -edge XANES spectra measured at room temperature on a series of REFeAsO (RE = La, Pr, Nd and Sm) samples. The L_3 edge XANES spectra are characterized by a strong white line, typical of trivalent RE [19–22], that could be fairly described using

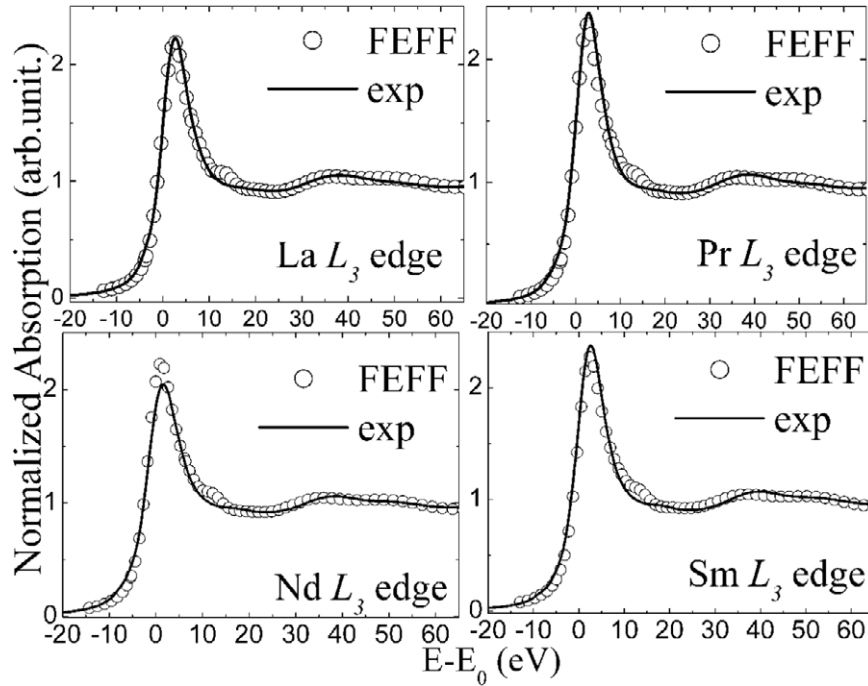


Figure 2. FEFF calculations (open circles) of the L_3 -edge for the REFeAsO (RE = La, Pr, Nd, Sm) system compared with the experimental spectra (solid lines).

the one electron picture. In the figure one can identify four distinct features; the white line feature A reflects directly the transition from core p electrons to partial empty d states, while features C and D originate from multiple scattering contributions, the so called shape resonances. Feature B has different intensity for different RE systems and appears to be related to the electronic structure. The white line intensities hardly show any systematic change with the RE size, while features C and D change systematically due to changing bond lengths [27]. It should be mentioned that a direct comparison of the white line intensities is impossible unless complete information on the transition matrix element is available in addition to the experimental artifacts. On the other hand, the relative variation of peaks C and D appears to follow the vertical position of the As atoms with respect to the Fe-Fe plane [16, 27], controlling the superconductivity (while the system is doped) and magnetic moment (undoped) of these materials. In addition, the weak feature B also appears to show a systematic change with varying rare-earth size. It should be recalled that a similar feature B has been seen in the L_3 -edge XANES measured on cuprates, however, discussed in the past with a dubious interpretation based on two types of structural symmetries [28, 29]. Since the average structural symmetry of the REFeAsO does not change with the RE, it is possible that feature B is due to the electronic structure and/or due to a local disorder in the REO layers. Moreover, the intensity of this feature appears to scale with the superconducting transition temperature (while the system is doped), and hence it should be interesting to address feature B in detail.

Let us first discuss the electronic structure. The electronic configuration of La ($[\text{Xe}]5d^16s^2$) does not have any f electrons in the ground state, while the number of f electrons increases

up to six in that of samarium, with the electronic configurations being $[\text{Xe}]4f^36s^2$, $[\text{Xe}]4f^46s^2$ and $[\text{Xe}]4f^66s^2$ for Pr, Nd and Sm, respectively. This suggests a non-negligible role for the 4f electrons in the L_3 -edge XANES spectra. Indeed, the ground state atomic configuration effect is negligible in most of the K edges, but can be significantly important in the L_3 -edge of rare-earth metals, well recognized in the Ce L_3 -edge of CeO_2 [30]. As a matter of fact, the one electron approach with muffin-tin approximation could reproduce reasonably well the RE L_3 edge XANES for all the rare-earth atoms in the REFeAsO, albeit with a clear disagreement for feature B. Indeed, the one electron calculations reveal a distinct feature B unlike the experimental spectra in which the feature appears damped (figure 2). Differences between the experimental and theoretical spectra could be due to the convolution function accounting for the intrinsic core-hole lifetime, and the extrinsic experimental resolution can be ruled out since the L_3 -edge energies for all the RE lies within an energy interval of about 1500 eV. In addition, there appears a small discrepancy in the peak position of feature B. The fact that we have used average crystallographic ordered structural parameters for the calculations makes it difficult to expect a perfect match of the energy position, since local structure disorder and defects can easily change the energy position. To have further insight, it is useful to compare the density of states (DOS) calculations illustrating the electronic structure of the system.

Figure 3 shows the DOS projected on the rare-earth atoms. We have used the ground state configuration for the calculations (no core hole), consistently with the one electron RE L_3 -edge XANES (figure 2). The DOS shows that the near edge absorption intensity in the RE L_3 -edge XANES spectra is mainly given by the transition from the 2p to 5d states. Near

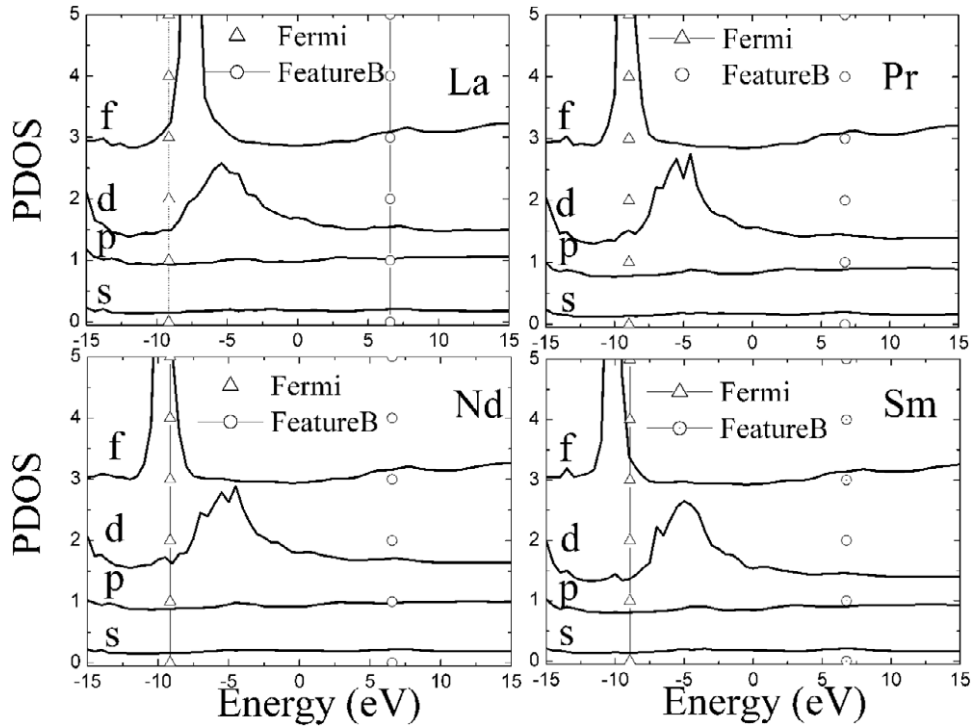


Figure 3. Projected electronic density of states on the central absorber RE metal atoms in the REFeAsO (RE = La, Pr, Nd, Sm) system. The triangles and circles are to guide energy positions of the Fermi level and the feature B, respectively.

the Fermi level, most of the 4f DOS of lanthanum are empty, while the 4f DOS becomes increasingly occupied as the atomic number of the RE increases. Feature B in the L_3 -edge XANES could probe the empty 4f electron states, however, a direct transition from 2p states to 4f final states is not allowed. On the other hand, from the projected DOS on other atoms (e.g. Fe, As or O), shown in figure 4, it appears that the iron empty p states mainly contribute to feature B. Therefore feature B probes the hybridization of RE 4f states and Fe 4p states. Nevertheless, we should mention that the RE 4f states and the Fe 4p states do not vary significantly with changing RE with experimental observation, suggesting that the electronic structure alone may not be able to explain feature B, and that multiple scattering contributions should be taken into account.

Figure 5 shows RE L_3 -edge XANES multiple scattering calculations for two representative REFeAsO (RE = La, Sm) systems with an increasing number of atomic shells around the absorbing atom. The atomic potential is calculated over a large cluster (~ 8 Å) of atoms and fixed self-consistently. Details on different shells around the absorbing RE (La, Sm) atoms are provided in table 1 with corresponding inter-atomic distances and coordination numbers.

From multiple scattering calculations of the La and Sm L_3 -edges, we can notice that feature B emerges and evolves in similar way for both La and Sm. The results of the calculations can be summarized as follows:

- (i) feature B emerges due to the constructive interference between multiple scattering waves when the cluster increases up to five shells with the addition of four RE (La or Sm) atoms in the same plane as the absorber;

Table 1. The model cluster used for the simulations at the L_3 -edge of RE metals in the REFeAsO (RE = La, Pr, Nd, Sm) system.

L_3 edge	La (Z = 57)	Pr (Z = 59)	Nd (Z = 60)	Sm (Z = 62)
T_c (K) ^a	25.9	43.2	50.9	52.8
Energy (eV)	5483	5964	6208	6716
1st shell	4O (2.35 Å)	4O (2.34 Å)	4O (2.29 Å)	4O (2.28 Å)
2nd shell	4As (3.37 Å)	4As (3.36 Å)	4As (3.28 Å)	4As (3.28 Å)
3rd shell	4Fe (3.72 Å)	4Pr (3.72 Å)	4Nd (3.64 Å)	4Sm (3.61 Å)
4th shell	4La (3.75 Å)	4Fe (3.74 Å)	4Fe (3.66 Å)	4Fe (3.68 Å)
5th shell	4La (4.02 Å)	4Pr (4.02 Å)	4Nd (3.94 Å)	4Sm (3.94 Å)
6th shell	As (4.25 Å, 4.45 Å)	As (4.20 Å, 4.50 Å)	As (4.08 Å, 4.44 Å)	As (4.02 Å, 4.50 Å)
7th shell	8O (4.66 Å)	8O (4.65 Å)	8O (4.56 Å)	8O (4.56 Å)
8th shell	8Fe (5.48 Å)	8Fe (5.49 Å)	8Fe (5.38 Å)	8Fe (5.40 Å)
9th shell	4La (5.69 Å)	4Pr (5.69 Å)	4Nd (5.58 Å)	4Sm (5.58 Å)
10th shell	4As (5.85 Å)	4As (5.81 Å)	4As (5.67 Å)	4As (5.63 Å)
11th shell	4Fe (5.93 Å)	4Fe (5.90 Å)	4Fe (5.78 Å)	4Fe (5.75 Å)
12th shell	4As (6.0 Å)	4As (6.04 Å)	4As (5.94 Å)	4As (5.98 Å)
13th shell	4O (6.16 Å)	4O (6.15 Å)	4O (6.03 Å)	4O (6.03 Å)

^a The maximum T_c while the system is doped.

- (ii) intensity of feature B increases with the addition of two As atoms on the top and the bottom, with the feature getting sharper when eight oxygen atoms at a distance ~ 4.6 Å are added in the REO slab (see the 7th shell in the table 1). This suggests a significant role for the oxygen shell on feature B;
- (iii) feature B disappears as the plane of eight iron atoms (see the 8th shell, at ~ 5.40 Å) is included in the calculation. These iron and oxygen atoms of the 7th shell have the same x and y coordinates but are located on the lower

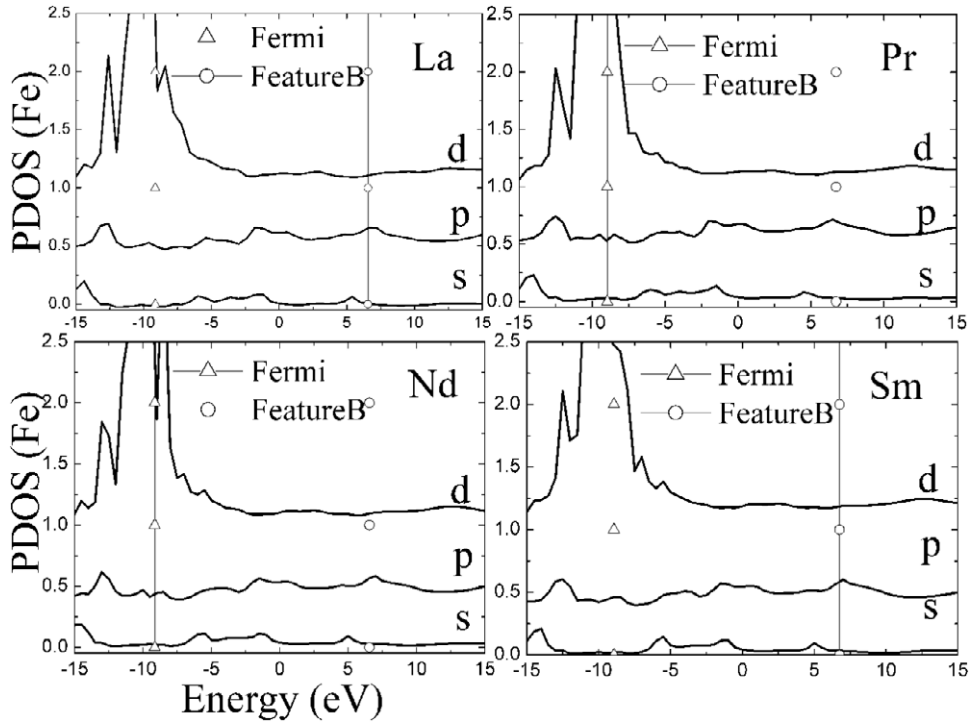


Figure 4. Projected electronic density of states on the iron atom in the REFeAsO (RE = La, Pr, Nd, Sm) system. The triangles and circles are to guide energy positions of the Fermi level and the feature B, respectively.

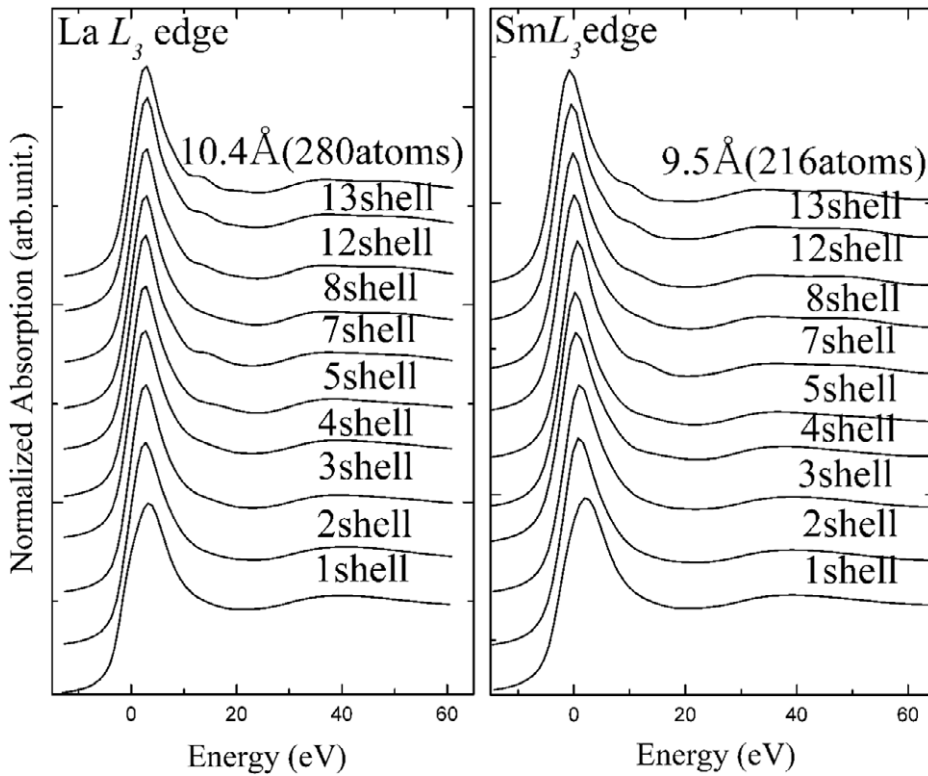


Figure 5. Multiple scattering calculations of the L_3 -edge with varying shell size.

side of the absorber. Since feature B disappears, the electron waves scattered by the iron plane (8th shell) and the oxygen plane (7th shell) should interfere destructively; (iv) feature B reappears if more atomic shells are included, suggesting that it is associated to the layered structure.

The fact that the peak intensities for La and Pr are much smaller, the oxygen layer with respect to the Fe plane should be less disordered in the LaFeAsO and PrFeAsO systems. However, multiple scattering contributions from atoms up to 6 Å actively contribute to feature B.

In the high temperature cuprate superconductors, a similar feature appearing in the RE L_3 edges was intensively investigated [28, 29] and found to be related to the eightfold hexahedron-type coordination surrounding the absorber. The only difference between cuprates and the iron pnictides is that there is no CuO_2 like plane in the latter. Both the REO and FeAs layers are slabs (Fe and As are not in the same plane) rather than planes. Moreover, the calculated spectra show a strong intensity of feature B, for a significantly large cluster of atoms, regardless of type of the rare-earth absorber. However, in the experimental spectra, the intensity of feature B increases with increasing atomic number. On the basis of the electronic structure and the multiple scattering calculations, we argue that feature B should be due to; (a) the hybridization between the RE 4f and Fe 4p states, which increases with an increase in the number of f electrons, and; (b) the multiple scattering of iron and oxygen layers sandwiching the layer of rare-earth metals. The latter suggests that oxygen disorder may significantly affect the intensity of feature B, as observed in the experimental spectra. It is worth recalling that any change in the local symmetry could create a structure in the XANES, as shown in the Ni K edge of PrNiO_3 system [31]. Since relative disorder between the FeAs and REO blocks indicates changing local symmetry, the findings are not inconsistent.

It is worth recalling that multiple electron excitations (MEE) could also produce a structure in the XANES spectrum. For example, a double excitation is identified in the Cu K edge x-ray absorption of cuprates [32], appearing around 85 eV above the 1s threshold, characterized by a simultaneous excitation of the 1s and 3p electrons into unoccupied states leaving two holes on the Cu site. Considering that feature B in the RE L_3 -edge XANES appears around 15 eV above the threshold, in principle a double electron excitation could be associated to $\text{O}_2(5p_{1/2})$ and $\text{O}_3(5p_{3/2})$ transitions, since for the light RE (such as Ce, Pr, Nd, Sm etc) these transitions fall in the range of 15–22 eV [33]. However, as discussed in [33], the main contribution of double excitation in the RE L_3 edges comes from the $L_3N_{4,5}$ excitations, and other potential contributions are very weak. Therefore, we can rule out feature B being due to an MEE.

Here, we should also underline that the misfit strain between the REO and the FeAs slabs could easily control the order/disorder of the oxygen, of which the mobility depends on the misfit strain. In SmFeAsO , the FeAs slabs are less strained, while the vertical position of the As atoms is higher [16], with a high interlayer coupling and hence more disordered positions of O atoms. On the other hand, the vertical position of the As atoms is lower in the case of LaFeAsO and the intensity of feature B may be lowered due to a destructive multiple scattering interference derived from higher order in the REO slabs, unlike the case of SmFeAsO , in which is the disorder could increase the multiple scattering contributions. The results are consistent with the fact that feature B is sensitive to the doping, being more intense for F substitution (in place of O) [27], and hence increased (chemical) disorder in the REO slabs. It is interesting to compare the results with the crystallographic structural phase transition in the REFeAsO system. The structural phase transition from the tetragonal

to the orthorhombic phase appears at 165 K, 155 K, 135 K and 130 K respectively for RE = La, Pr, Nd and Sm. This implies that a larger relative interlayer disorder reduces the structural phase transition temperature. This seems reasonable since local disorder can easily destroy the average symmetry.

In summary, we have investigated RE L_3 -edge XANES of the REFeAsO system. The L_3 -edge shows a feature B (see figure 1) evolving from weak, for the lower Z lanthanide (La and Pr), to intense, for the higher Z lanthanides metal (e.g., Nd and Sm). From detailed DOS and multiple scattering calculations, we claim that this feature is not only related to the electronic configuration of the rare-earth metals, but also to multiple scattering contributions originating from the geometrically symmetric oxygen and iron positions. This suggests that the oxygen should be less disordered with respect to the Fe layer in LaFeAsO , while there is a significant oxygen disordering due to a higher interlayer coupling (higher vertical position of the As atoms) and a smaller misfit strain [5, 7] in the SmFeAsO system. Since, once suitably doped, the superconducting transition temperature of SmFeAsO is higher than LaFeAsO , the present results suggest an intimate relation or an interplay between the superconductivity and disorder in the spacer layers, similar to the out-of-plane disorder controlled superconductivity addressed in the cuprate superconductors [9, 10].

Acknowledgments

The authors thank the Elettra staff for their help and cooperation during the experimental run. We also acknowledge Z X Zhao and Z A Ren (Beijing) for providing high quality samples for the present study. This work was partly supported by the National Outstanding Youth Fund (Project No. 10125523 to ZW) and by the Knowledge Innovation Program of the Chinese Academy of Sciences (KJXC2-YW-N42). We gratefully acknowledge the support of the Italian Ministry of Foreign Affairs in the framework of the 12th Executive Program of Scientific and Technological Cooperation between the Italian Republic and the People's Republic of China. In particular one of the authors (WX) acknowledges the financial support from the Italian Ministry of Foreign Affairs; and he is grateful to Dr Dongliang Chen for the fruitful discussions in using the FEFF code.

References

- [1] Kamihara Y, Watanabe T, Hirano M and Hosono H 2008 *J. Am. Chem. Soc.* **130** 3296
- [2] Ishida K, Nakai Y and Hosono H 2009 *J. Phys. Soc. Japan* **78** 062001
- [3] Tokura Y and Arima T 1990 *Japan. J. Appl. Phys.* **29** 2388
- [4] Goodenough J B 2004 *Rep. Prog. Phys.* **67** 1915
- [5] Rodgers J A, Penny G B S, Marcinkova A, Bos J-W G, Sokolov D A, Kusmartseva A, Huxley A D and Atfield J P 2009 *Phys. Rev. B* **80** 052508
- [6] Billinge S J L and Duxbury P M 2002 *Phys. Rev. B* **66** 064529
- [7] Ricci A, Poccia N, Ciasca G, Fratini M and Bianconi A 2009 *J. Supercond. Nov. Magn.* **22** 589
- [8] Hess C, Kondrat A, Narduzzo A, Hamann-Borrero J E, Klingeler R, Werner J, Behr G and Büchner B 2009 *Europhys. Lett.* **87** 17005

- [9] Gao W B, Liu Q Q, Yang L X, Yu Y, Li F Y, Jin C Q and Uchida S 2009 *Phys. Rev. B* **80** 094523
- [10] Eisaki H, Kaneko N, Feng D L, Damascelli A, Mang P K, Shen K M, Shen Z-X and Greven M 2004 *Phys. Rev. B* **69** 064512
- Fujita K, Noda T, Kojima K M, Eisaki H and Uchida S 2005 *Phys. Rev. Lett.* **95** 097006
- [11] Bianconi A, Bianconi G, Caprara S, Di Castro D, Oyanagi H and Saini N L 2000 *J. Phys.: Condens. Matter* **12** 10655
- Bianconi A, Agrestini S, Bianconi G, Di Castro D and Saini N L 2001 *J. Alloys Compounds* **317** 537
- Agrestini S, Saini N L, Bianconi G and Bianconi A 2003 *J. Phys. A: Math. Gen.* **36** 9133
- [12] Ren Z A et al 2008 *Europhys. Lett.* **83** 17002
- [13] Lee C-H, Iyo A, Eisaki H, Kito H, Fernandez-Diaz M T, Ito T, Kihou K, Matsuhata H, Braden M and Yamada K 2008 *J. Phys. Soc. Japan* **77** 083704
- Miyazawa K, Kihou K, Shirage P M, Lee C-H, Kito H, Eisaki H and Iyo A 2009 *J. Phys. Soc. Japan* **78** 034712
- Lee C-H et al 2008 *J. Phys. Soc. Japan* **77** (Suppl. C) 44
- [14] Fratini M et al 2008 *Supercond. Sci. Technol.* **21** 092002
- [15] Margadonna S, Takabayashi Y, McDonald M T, Brunelli M, Wu G, Liu R H, Chen X H and Prassides K 2009 *Phys. Rev. B* **79** 014503
- Kasperkiewicz K, Bos J W G, Fitch A N, Prassides K and Margadonna S 2009 *Chem. Commun.* **707**
- [16] Iadecola A, Agrestini S, Filippi M, Simonelli L, Fratini M, Joseph B, Mahajan D and Saini N L 2009 *Europhys. Lett.* **87** 26005
- [17] Bianconi A, Dell'Ariceia M, Durham P J and Pendry J B 1982 *Phys. Rev. B* **26** 6502
- Bianconi A, Incoccia L and Stipcich S (ed) 1982 *EXAFS and Near Edge Structure* (Berlin: Springer)
- Bianconi A 1988 *X-Ray Absorption: Principles, Applications, Techniques of EXAFS, SEXAFS, XANES* ed R Prinz and D Koningsberger (New York: Wiley)
- [18] Benfatto M, Natoli C R, Bianconi A, Garcia J, Marcelli A, Fanfoni M and Davoli I 1986 *Phys. Rev. B* **34** 5774
- Natoli C R, Benfatto M, Della Long S and Hatada K 2003 *J. Synchrotron Radiat.* **10** 26
- [19] Journel L et al 2002 *Phys. Rev. B* **66** 045106 and references therein
- [20] Bianconi A, Marcelli A, Karnatak R, Dexpert H, Kotani A, Jo T and Petiau J 1987 *Phys. Rev. B* **35** 806
- [21] Fukui K, Ogasawara H, Kotani A, Harada I, Maruyama H, Kawamura N, Kobayashi K, Chaboy J and Marcelli A 2001 *Phys. Rev. B* **64** 104405
- [22] Chaboy J, Piquer C, Marcelli A, Battisti M, Cibin G and Bozukov L 1998 *Phys. Rev. B* **58** 77
- Chaboy J, Garcia J and Marcelli A 1997 *J. Magn. Magn. Mater.* **166** 149
- Chaboy J, Marcelli A and Bozukov L 1995 *J. Phys.: Condens. Matter* **7** 8197
- Chaboy J, Marcelli A, Bozukov L, Baudelet F, Dartyge E, Fontaine A and Pizzini S 1995 *Phys. Rev. B* **51** 9005
- [23] Ren Z-A et al 2008 *Europhys. Lett.* **82** 57002
- [24] Ankudinov A L, Ravel B, Rehr J J and Conradson S D 1998 *Phys. Rev. B* **58** 7565
- [25] Ankudinov A L, Nesvizhskii A I and Rehr J J 2003 *Phys. Rev. B* **67** 115120
- Moreno M S, Jorissen K and Rehr J J 2007 *Micron* **38** 1
- [26] Hedin L and Lundqvist S 1970 *Solid State Physics* vol 23, ed D T Frederick Seiz and E Henry (New York: Academic) p 1
- [27] Joseph B, Iadecola A, Fratini M, Bianconi A, Marcelli A and Saini N L 2009 *J. Phys.: Condens. Matter* **21** 432201
- [28] Tan Z, Filipkowski M E, Budnick J I, Heller E K, Brewé D L, Chamberland B L, Bouldin C E, Woicik J C and Shi D 1990 *Phys. Rev. Lett.* **64** 2715
- Tan Z, Budnick J I, Chen W Q, Brewé D L, Cheong S-W, Cooper A S and Rupp L W 1990 *Phys. Rev. B* **42** 4808
- Tan Z, Budnick J I, Luo Sheng, Chen W Q, Cheong S-W, Cooper A S, Canfield P C and Fisk Z 1991 *Phys. Rev. B* **44** 7008
- Tan Z, Heald S M, Cheong S-W, Cooper A S and Budnick J I 1992 *Phys. Rev. B* **45** 2593
- [29] Wu Z Y, Benfatto M and Natoli C R 1992 *Phys. Rev. B* **45** 531
- Wu Z Y, Benfatto M and Natoli C R 1998 *Phys. Rev. B* **57** 10336
- [30] Soldatov A V, Ivanchenko T S, Della Longa S, Kotani A, Iwamoto Y and Bianconi A 1994 *Phys. Rev. B* **50** 5074
- [31] Acosta-Alejandro M, Mustre de Leon J, Medarde M, Lacorre Ph, Conder K and Montano P 2008 *Phys. Rev. B* **77** 085107
- [32] Di Cicco A and Sperandini F 1996 *Physica C* **258** 349
- [33] Chaboy J, Marcelli A and Tyson T A 1994 *Phys. Rev. B* **49** 11652
- Chaboy J, Garcia J, Marcelli A and Tyson T A 1993 *Japan. J. Appl. Phys.* **32** 61
- Chaboy J, Garcia J, Marcelli A and Ruiz Lopez M F 1990 *Chem. Phys. Lett.* **174** 389